Korean J. Chem. Eng., **30**(5), 1013-1022 (2013)
DOI: 10.1007/s11814-013-0035-6

Effect of organoclay on non-linear rheological properties of poly(lactic acid)/poly(caprolactone) blends

Reza Salehiyan and Kyu Hyun†

School of Chemical and Biomolecular Engineering, Pusan National University, Busan 609-735, Korea
(*Received 6 November 2012 • accepted 3 March 2013*)

Abstract−The nonlinear viscoelastic properties of PLA/PCL blends with and without clay (montmorillonite, MMT) under large amplitude oscillatory shear (LAOS) flow were investigated. The G′ and G″ as a function of strain amplitude, Lissajous plots and FT-rheology methods were used to interpret nonlinear behavior of PLA/PCL blends with and without MMT. Additionally, scanning electron microscopy (SEM) images of PLA/PCL with MMT blends were taken to investigate the effects of clay on the internal structure of the PLA/PCL blends. A relationship between morphological changes and linear and nonlinear rheological properties was observed. SEM image analysis revealed that clay acted as a compatibilizer and then reduced the size of droplets in the PCL domain of the PLA matrix. As a result, nonlinear properties sensitively reflect morphological changes with increasing MMT amount. The nonlinear rheological properties of PLA/PCL/MMT/metallocene-LLDPE (mLLDPE) were also investigated when mLLDPE was used as an impact modifier to improve mechanical properties, and the nonlinear rheological properties of PLA/PCL/MMT and PLA/PCL/MMT/mLLDPE were also compared.

Key words: LAOS, Nonlinear Viscoelastic Properties, FT-rheology, PLA/PCL Blends, PLA/PCL/MMT, PLA/PCL/MMT/mLLDPE

INTRODUCTION

Polymers from renewable resources have attracted considerable attention over the last two decades, due to environmental concerns and the depletion of petroleum resources. The potential of these materials for use in medical devices, packaging, and automotive applications is currently being investigated by many researchers and industries [1,2]. One of the best candidate biopolymers is polylacticacid (PLA) due to its remarkable mechanical and thermal properties as well as its biodegradability [3,4]. However, its high brittleness limits its application to some extent [5]. PLA can be blended with other polymers with lower glass transition temperatures to overcome its brittleness. Polycaprolactane (PCL) and polyethyleneglycol (PEG) are plasticizers that can be blended with PLA [2,6]. However, these blends might weaken some properties of PLA, such as barrier, thermal and mechanical properties; hence, incorporation of fillers such as nano-particles into this blend system is needed to improve these characteristics [7-9].

One promising method of characterizing polymer blends is by rheological measurements, among which small amplitude oscillatory shear (SAOS) tests are most common [10,11]. Linear viscoelastic behavior is normally measured by the frequency sweep test within small amplitude ranges. Strain amplitude is required to be kept small enough to ensure the linear response. Storage modulus $G'(\omega)$ and loss modulus $G''(\omega)$ are material functions measured by SAOS tests to quantify elastic and viscous responses, respectively. SAOS tests are believed to provide a more reliable rheological response since they are based on strong mathematical backgrounds [10,11]. Many studies have focused on linear viscoelastic properties to investigate polymer blends or polymer composites. Therefore, a large number of investigations have been conducted to evaluate PLA blends and composites with linear rheological properties using SAOS tests. Ray et al. [2] studied linear rheological properties of PLA and PLA clay nanocomposites (PLA/MMT) and found significant storage modulus $G'(\omega)$ and loss modulus $G''(\omega)$ enhancements at low frequencies with increasing amounts of MMT. The G′ and G″ exhibited frequency independence at very low frequencies when PLA/MMT nanocomposites were used. A pseudo-solid-like behavior was observed for PLA nanocomposites since $G'(\omega)$ was higher than $G''(\omega)$ at low frequencies. Wu et al. [12] studied the linear viscoelastic behavior of PLA/PCL blends at different blend compositions to investigate the composition effect on linear rheological properties, and PCL concentration dependence on G′ and G″ was found. Both storage and loss moduli (G′&G″) decreased as the PCL content increased. However, when the PLA content was 70 and 80 wt%, the nonterminal region was higher than that of neat PLA. They suggested that phase inversion could occur between 60% and 70 wt% PLA content, which was confirmed by SEM images of the blends. In another study, they investigated the effect of diblock PLA-b-PCL and triblock PCL-PLA-PCL as compatibilizers on a 70 wt% PLA/30 wt% PCL blend using SAOS measurement. Their findings indicated that higher compatibilizer content resulted in higher nonterminal regions at low frequencies. In other words, higher compatibilizer content produces higher elasticity at low frequencies. A Palierne model was used to calculate the interfacial tensions and the results showed that both diblock and triblock copolymers significantly reduced the interfacial tensions. However, triblock copolymer was more effective at emulsifying the PLA/PCL blend corresponding to its higher LA (Lactic Acid) concentration [13]. Later, the effects

†To whom correspondence should be addressed.
E-mail: kyuhyun@pusan.ac.kr

of organoclay (modified montmorillonite with methyl tallow bis-(2-hydroxyethyl) ammonium also known as DK2) on the linear viscoelastic properties of the PLA/PCL (80/20) blends were investigated by Sabet et al. [14]. An increase in storage modulus and loss modulus was observed upon clay incorporation at low frequencies and non-terminal behavior was more pronounced at higher clay contents. In another study, the effects of clay as nano-particles on linear rheological properties of PLA were investigated by Ahmed et al. [15]. Similar enhancements were reported as the clay concentration increased; however, viscous-like-behavior was observed at low frequencies below 9 wt% clay. Moreover, they added polyethyleneglycol (PEG) to the PLA matrix as a plasticizer and both storage and loss moduli of the corresponding blend decreased significantly as a result of the plasticizing effect of PEG. Recently, Li et al. [16] investigated the effect of a PLA/PBAT (poly butylenes adipate-co-terephtalate) blend on linear rheological properties. Complex viscosity (η^*) as a function of frequency increased when PBAT concentration increased; however, Newtonian behavior decreased, indicating stronger shear-thinning behavior of PBAT. Similar to the complex viscosity, $G'(\omega)$ at low frequencies increased as the PBAT content increased up to 20 wt%. With the PBAT content increasing more than 20 wt%, however, $G'(\omega)$ at low frequencies decreased. Overall, their results suggested that the PLA/PBAT blend has the highest entanglement at the optimum level composition of 80 wt%/20 wt%, which led to the highest modulus at this composition.

Despite the usefulness of the linear rheological properties in characterizing complex fluids, there is still some controversy over the sufficiency of the SAOS test for probing the materials' viscoelastic properties. In practical situations, deformations are large and no longer within the linear regime; thus, the response of the material falls into a nonlinear regime. Accordingly, it is necessary to investigate the nonlinear rheological properties of the complex fluids to investigate the effects of microstructural changes as they are known to be interrelated.

For higher resolution of nonlinear response at higher deformations, large amplitude oscillatory shear (LAOS) tests are applicable as strain amplitudes, and frequency can be controlled independently. Moreover, LAOS tests are sensitive to any internal change in morphology, topology and concentration of the second dispersed phase into the medium, therefore, LAOS can be used as a powerful tool to investigate the microstructure and internal structure of complex materials [17-27]. Strain sweep tests are used to quantify nonlinear viscoelasticity using storage modulus $G'(\gamma)$ and loss modulus $G''(\gamma)$ in which both moduli are a function of strain amplitude. Strain sweep tests can provide useful insights into the material's transition from linear region to nonlinear.

The material is applied to large sinusoidal deformations; the stress response of material is no longer sinusoidal. Therefore, a variety of analysis methods have been suggested by several researchers [27]. Wilhelm et al. [28] introduced Fourier transform rheology (FT-Rheology) as a new method to characterize nonlinear stress curves under a nonlinear regime. Specifically, they used Fourier transform to convert distorted periodical signals (nonlinear stress) in the time domain to intensity signals in frequency domains. The outcome was the appearance of odd higher harmonics in intensity signals at nonlinear regions. Therefore, it is believed that FT-Rheology is a powerful tool to quantify the distorted stress curves of complex fluids under LAOS flow. The effects of different compatibilizers on rheological properties of liquid crystalline polymer (LCP)/Olefinic thermoplastic (TP) blends along the extruder length were investigated by Filipe et al. [29], using both SAOS and LAOS tests. They pointed out that even though SAOS tests could discriminate the different microstructures, but LAOS and FT-Rheology tests were more sensitive to structural evolutions along the extruder length. Carotenuto et al. [30] investigated the nonlinear rheological properties of a dilute immiscible blend of (poly dimethylesiloxane) (PDMS) in (poly isobutylene) (PIB) under LAOS flow. They used FT-Rheology to probe the nonlinearity of the blend. The results revealed that the third relative intensity ($I_3/I_1 \equiv I_{3/1}$) of the blends showed significant dependence on strain amplitude. Furthermore, they noted that the FT-Rheology method could be used to distinguish morphological changes when they examined three different PDMS/PIB blends with different droplet sizes. Different droplet sizes gave rise to different ($I_{3/1}$) and ($I_{5/1}$) curves; however, the same trend was reported for all.

We used LAOS tests to characterize the effects of clay (MMT) on PLA/PCL blends. As mentioned above, some studies have investigated the linear viscoelastic properties of PLA/PCL blends and their nanocomposites (PLA/PCL/MMT). To the best of our knowledge, few studies have discussed the nonlinear rheological properties of PLA/PCL blends with and without MMT under LAOS flow. Therefore, our main objective was to investigate the effects of clay on the non-linear rheological characteristics of PLA/PCL blends under LAOS flow. Furthermore, the effects of MMT on PLA/PCL/metallocene catalyzed-LLDPE (Linear Low Density Polyethylene, mLLDPE) blends were investigated based on the nonlinear rheological properties.

EXPERIMENTAL

1. Materials

Polylacticacid (PLA labeled L9000, Mw: 220 KDa; Mn: 101 KDa) was supplied by Biomer (Germany). Polycaprolactone (PCL, Mw= 80,000 and density=1.08-1.12 g/cm^3 at 25 °C and a grade name= 800c) was purchased from Shenzhen Brightchina Industrial Co. (China). A hexane copolymer of Metallocene Linear Low Density Polyethylene (mLLDPE, Exceed 1018CA) was obtained from ExxonMobil Chemical's EXXPOL® Technology (USA). The mLLDPE has a density of 0.918 g/cm^3 and a melt index (MI) of 1 g/10 min. The organoclay (Nanomer 1.30TC) is a commercial product from Nanocor Inc. (IL, USA). This organoclay is a white powder containing montmorillonite (MMT, 30 wt%) intercalated by octadecylamine (30 wt%). The mean dry particle size of the organoclay is 16-22 μm.

2. Blends Preparation

Prior to compounding PLA, PCL and mLLDPE were dried at 40 °C, while MMT was dried at 100 °C for 24 hrs. All blends were compounded using Brabender Plasticoder (PL 2000) a counter rotating twin-screw extruder, and a 70/30 blend ratio (wt%) of the PLA/PCL was selected. MMT and mLLDPE were added to the blend in parts per hundred (phr). Specifically, the MMT contents used were 1, 2 and 4 phr, while the content of mLLDPE was fixed at 10 phr. Compounding was conducted at an average temperature of 190 °C along the extruder from the feed section to the die head through a decreasing temperature profile at a fixed screw speed of 30 rpm.

Table 1. Materials designation, compositions

Designation	Composition	Parts
PLA/PCL	PLA/PCL	70/30
PLA/PCL/MMT1	PLA/PCL/MMT	70/30/1
PLA/PCL/MMT2	PLA/PCL/MMT	70/30/2
PLA/PCL/MMT4	PLA/PCL/MMT	70/30/4
PLA/PCL/ mL10/MMT1	PLA/PCL/mLLDPE/MMT	70/30/10/1
PLA/PCL/ mL10/MMT2	PLA/PCL/mLLDPE/MMT	70/30/10/2
PLA/PCL/ mL10/MMT4	PLA/PCL/mLLDPE/MMT	70/30/10/4

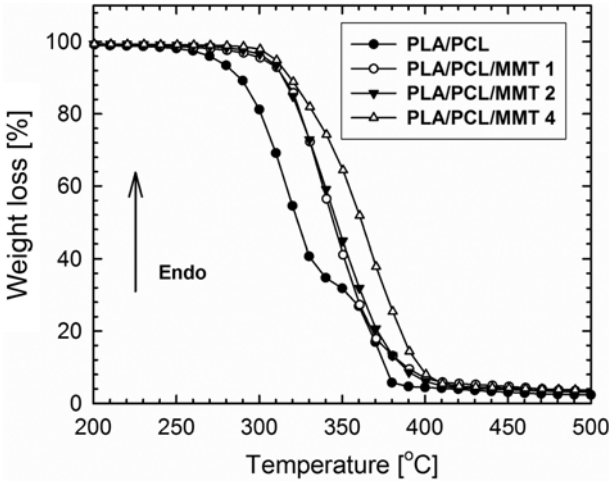

Fig. 1. Thermogravimetry analysis of PLA/PCL and PLA/PCL/MMT blends under nitrogen atmosphere at heating rate of 10 °C/min.

Table 1 show the materials used in this study.

3. Thermal Analysis

To find a safe temperature range to prevent any possible thermal degradation, thermogravimetry analysis (TGA) tests of PLA/PCL/MMT blends were carried out via a TGA/SDT851e (Mettler Toledo AG, Switzerland) under a nitrogen atmosphere. Samples were heated from 30 to 600 °C at a heating rate of 10 °C/min. Results from Fig. 1 indicate that onset of degradation of the blends occurred beyond 250 °C. Therefore, the experimental temperature of 190 °C was chosen, making sure that there was no thermal degradation at 190 °C.

4. Rheological Measurement

Sample discs with a 1 mm thickness and 25 mm diameter were made using a compressor molding machine at 190 °C. Rheological measurements were carried out on a strain controlled rheometer (RDA II, Rheometrics Scientific) using a 25 mm parallel plate geometry with a 1 mm gap. Strain sweep tests were carried out from strain amplitude γ_0=0.01 to 5 at a fixed frequency ω=1 rad/s. All experiments were conducted at 190 °C. To convert all data to signal forms a 16 bit ADC card (analog digital converting) was used together with the LabView software.

5. Morphology

JEOL JSM-6390 LV scanning electron microscopy (SEM) was used to observe the morphology of the blends. Samples were coated with a thin layer of platinum prior to examination under the electron beam with an operating voltage of 15 kV.

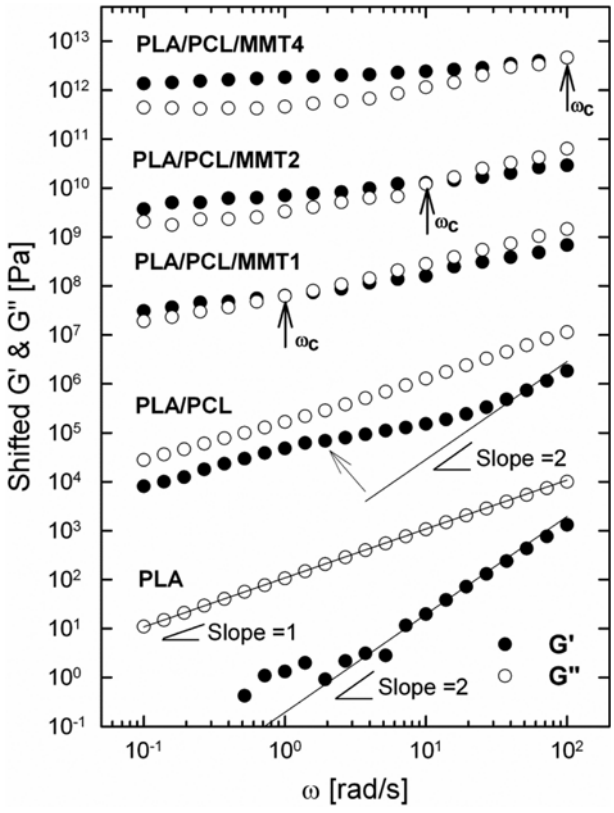

Fig. 2. Small amplitude oscillatory shear (SAOS) tests of PLA, PLA/PCL and PLA/PCL/MMT blends at a fixed strain amplitude γ_0=0.01 at 190 °C. The moduli data have been artificially shifted by 10^0 (PLA) 10^2 (PLA/PCL), 10^5 (PLA/PCL/MMT1), 10^7 (PLA/PCL/MMT2) and 10^9 (PLA/PCL/MMT4) respectively, for clarity of presentation. The arrows indicate crossover frequency ω_c, ω_c=100 rad/s for PLA/PCL/MMT4, ω_c=10 rad/s for PLA/PCL/MMT2, ω_c=1 rad/s for PLA/PCL/MMT1.

RESULTS AND DISCUSSION

1. SAOS and LAOS Tests for PLA/PCL/MMT Blends

SAOS (Small amplitude oscillatory shear) tests were performed at 190 °C and a fixed strain amplitude γ_0=0.01 within the linear regime. The effects of MMT amount on the linear rheological properties of PLA/PCL blends were investigated, and the linear rheological properties, G′ and G″, were found to show profound dependence on MMT amount as the initial moduli at low frequencies and crossover point shifted to higher frequency regions (ω_c=100 rad/s for PLA/PCL/MMT4, ω_c=10 rad/s for PLA/PCL/MMT2, ω_c=1 rad/s for PLA/PCL/MMT1) (see Figs. 2 and 3). At lower crossover frequencies, the storage modulus (G′) was larger than the loss modulus (G″). Wu et al. [31] investigated the viscoelastic properties of PLA/clay nanocomposites and concluded that formation of percolation structures is the main reason for the solid-like response of PLA/clay nanocomposites at low frequency ranges. Pure PLA and PLA/PCL blend show no crossover point (see Fig. 2). It indicated that addition of MMT gave rise to the solid-like behavior. In case of pure PLA, the classical behavior $G' \propto \omega^2$ and $G'' \propto \omega$ is observed in terminal regions, i.e., at low frequencies. However, PLA/PCL blend shows an upturn of G′ value at low frequencies from the classi-

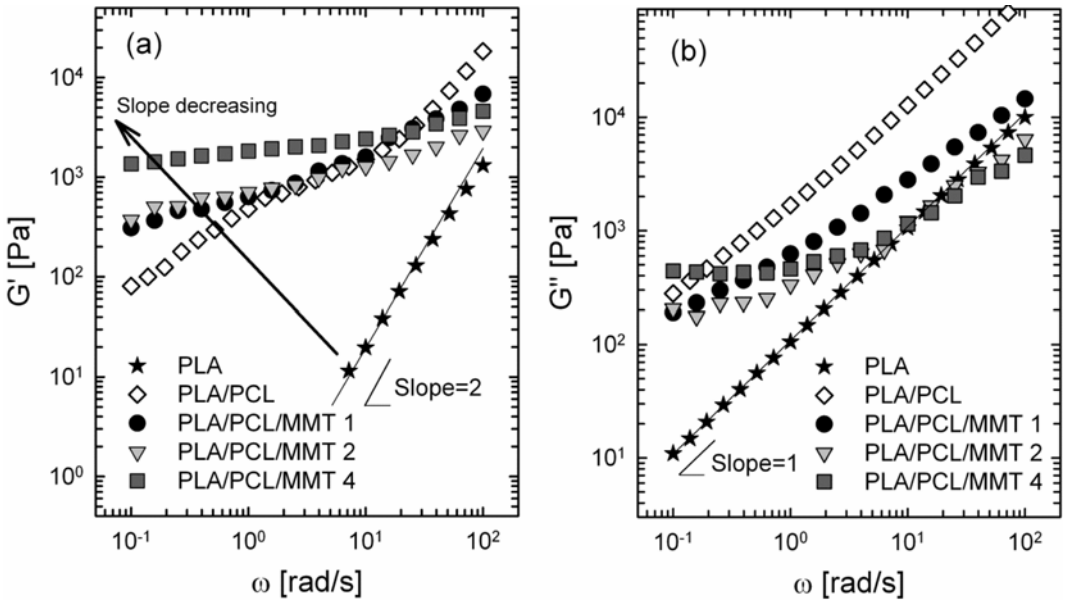

Fig. 3. Dynamic (a) storage modulus G′ and (b) loss modulus G″ of PLA/PCL blends at different MMT concentrations and fixed strain amplitude of 0.01 at 190 °C.

cal behavior $G' \propto \omega^2$, which is well known due to the interfacial contribution from immiscible blends. It means that the PLA/PCL blend has droplet phase. As the amount of MMT increases, the slope of G′ and G″ decreases (see Fig. 3). These results are consistent with the reduction of droplet size observed with addition of MMT.

SEM was used to evaluate the morphology and droplet size of the PCL dispersed phase in the PLA/PCL blend systems at different MMT concentrations (Fig. 4). All images show the droplet dispersion morphology taken from the fractured surface of PLA/PCL blends. Droplet sizes were calculated by SEM image analysis. The spherical dispersed PCL phase in the PLA matrix verified the immiscibility of PLA and PCL to some extent. The droplet size of the dispersed phase decreased when MMT was incorporated into the blend system (3.5±0.3 μm in PLA/PCL, 1.78±0.24 μm in PLA/PCL/MMT1, and 1.51±0.2 μm in PLA/PCL/MMT2). It can be inferred that MMT acted either as barrier to prevent coalescence of droplets by locating at interface or compatibilizer by reducing interfacial tensions between PCL droplets and the PLA matrix. Moreover, preferentially wetting either phases and changing the viscosity ratios could also be taking place to reduce the droplet sizes [14]. As shown

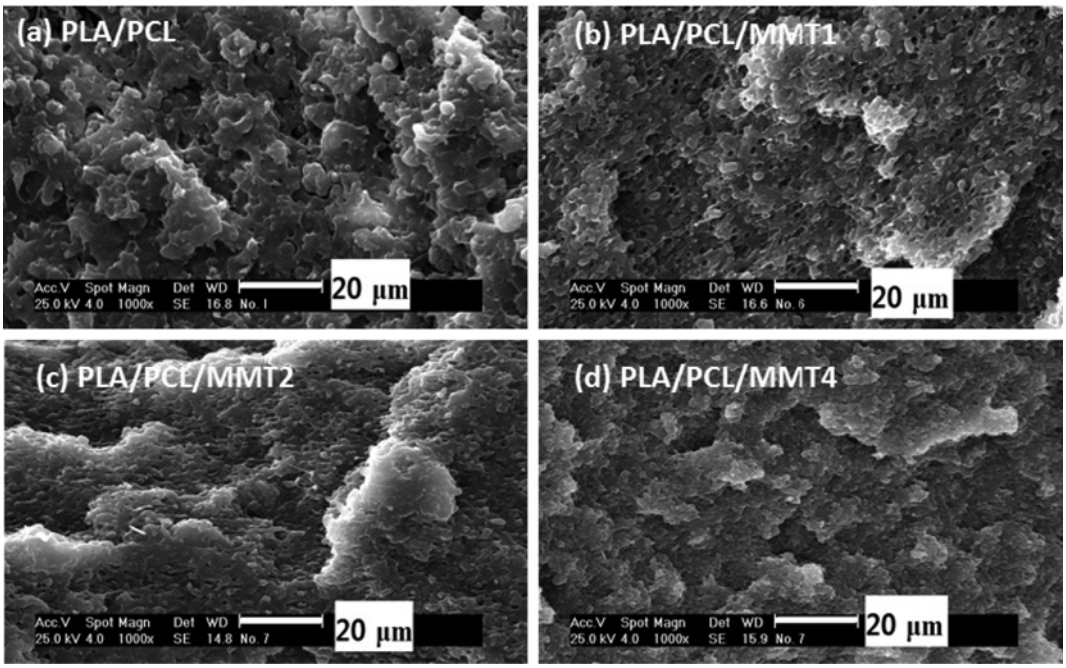

Fig. 4. SEM images of fractured surface of (a) PLA/PCL, (b) PLA/PCL/MMT1, (c) PLA/PCL/MMT2, (d) PLA/PCL/MMT4.

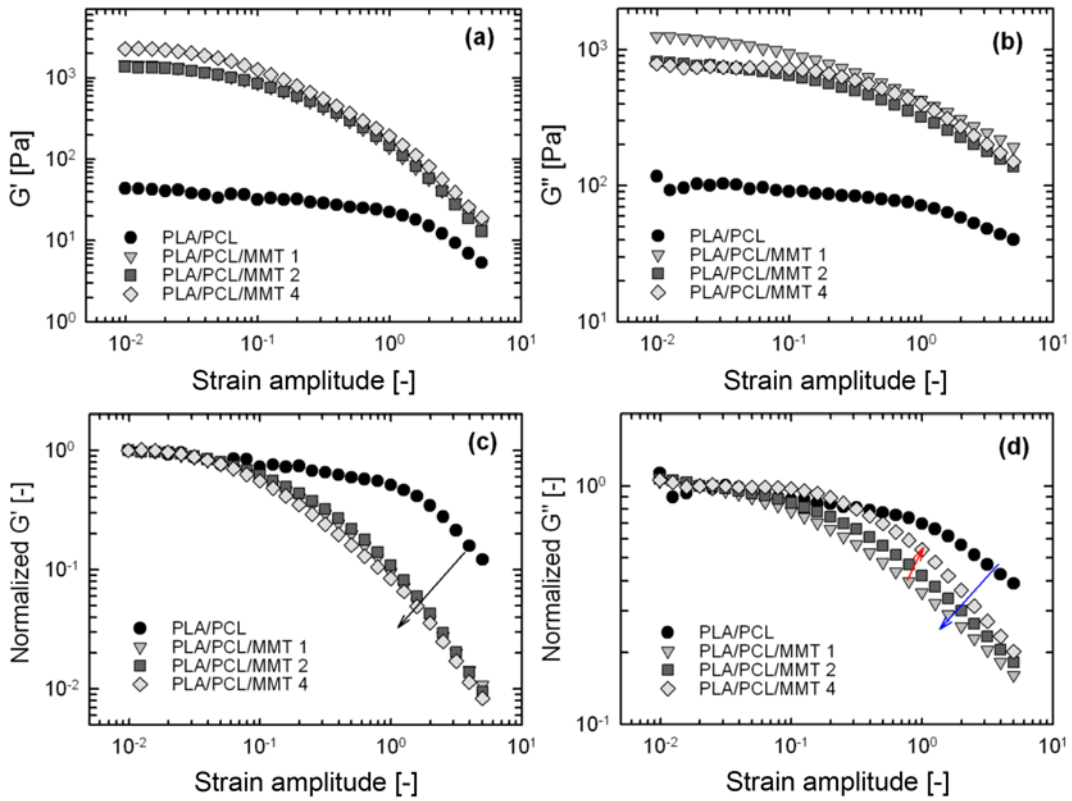

Fig. 5. Effect of MMT content on dynamic (a) storage modulus G′(γ), (b) loss modulus G″(γ), (c) normalized storage modulus [≡G′/G″ (linear regime)], and (d) normalized loss modulus [≡G″/G″ (linear regime)] of the PLA/PCL blends as a function of strain amplitude at a fixed frequency, ω=1 rad/s and 190 °C.

in Figs. 2 and 3, the SAOS data (both G′ and G″) show different trends with increasing MMT concentration because of decreasing droplet size.

LAOS (large amplitude oscillatory shear) tests were also conducted at 190 °C and a fixed frequency ω=1 rad/s. Fig. 5(a) and 5(b) illustrate the storage modulus G′ and loss modulus G″ as a function of strain amplitude from γ=0.01 to 5 for PLA/PCL and PLA/PCL/MMT. The storage (G′) and loss moduli (G″) increased significantly when MMT was introduced into the PLA/PCL blends. However, there was no profound change in the storage modulus of the PLA/PCL blends with clays (PLA/PCL/MMT) as the MMT content changed from 1 phr to 2 phr. Additionally, the G′(γ) of both PLA/PCL/MMT1 and PLA/PCL/MMT2 almost overlapped (see Fig. 5(a)). Conversely, the loss modulus (G″) of the PLA/PCL/MMT2 decreased slightly when the MMT content increased (see Fig. 5(b)). Moreover, the linear region shifted to the lower strain amplitudes when MMT was incorporated. This could have been due to the alignment of particles within the flow direction. It was also confirmed from normalized storage modulus [≡G′/G″ (linear regime)] of the blends in Fig. 5(c). As clay was added in the PLA/PCL blend, the PLA/PCL/MMT showed strain thinning at lower strain amplitude and stronger strain thinning behavior than PLA/PCL (see Fig. 5(c)). These findings indicate that MMT could accelerate the strain thinning of the blends as the strain amplitude is increased. Conversely, the normalized loss modulus [≡G″/G″ (linear regime)] maintained a constant value at a longer stain amplitude than PLA/PCL blends (see Fig. 5(d)). This phenomenon could be due to the well dispersed PCL domain in the PLA matrix with increasing clay content. The non-monotonic behavior of normalized loss modulus is consistent

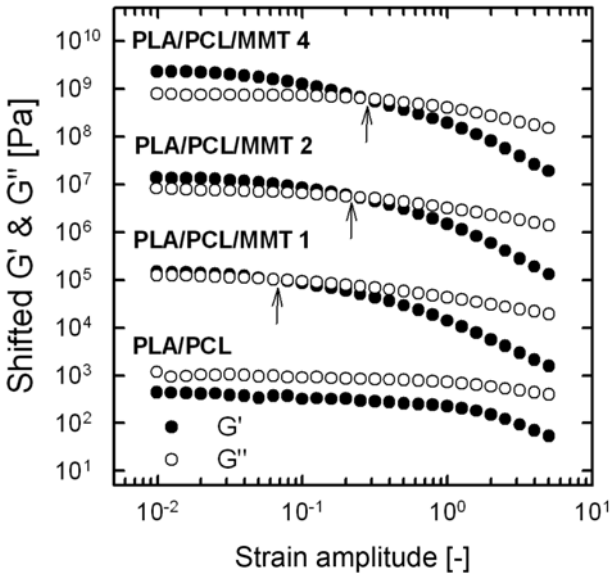

Fig. 6. The G′ and G″ as a function of strain amplitude at frequency ω=1 rad/s and 190 °C. The arrows indicate cross-over points (G′=G″). The moduli data have been artificially shifted by 10 (a) PLA/PCL, 10^2 (b) PLA/PCL/MMT1, 10^4 (c) PLA/PCL/MMT2, 10^6 (d) PLA/PCL/MMT4 respectively, for clarity of presentation.

with those results shown in Fig. 6, where crossover points shifted to larger strain amplitudes upon clay incorporations. Fig. 5 shows that addition of 1 phr clay increased the strain thinning behavior of G″ while addition of more clays decreased this phenomenon. Complex fluids were classified into the four following categories by Hyun et al. [21]: Type 1: strain thinning (both G′ and G″ decreases); Type 2: strain hardening (both G′ and G″ increase); Type 3: weak strain overshoot (G′ decreases and G″ increases up to a certain level of strain amplitudes and then decreases); and Type 4: strong strain overshoot (both G′ and G″ increase and then decrease). The results showed that both PLA/PCL blend systems showed Type 1 behavior (strain thinning). The effects of MMT content can be discussed from another point of view as they are illustrated in Fig. 6. In the case of the PLA/PCL blend, the G′ and G″ curves do not intersect each other and the loss modulus is higher than the storage modulus throughout the strain amplitude ranges, indicating that viscous-like behavior is dominant throughout the strain amplitude. When clays are added to the blend systems, the initial storage modulus gradually shifts to higher values than those of the loss modulus within the linear region up to a certain strain amplitude level, where they intersect each other (crossover strain amplitude γ_{0c}). This increase in the gap between G′ and G″ as a function of MMT content indicates enhancement of dominant solid-like behavior below the crossover point. Moreover, this crossover point shifts to larger amplitudes from γ_{0c}=0.06 at 1 phr MMT to 0.32 at 4 phr MMT. This enhancement in solid-like behavior upon MMT concentration could be due to the development of clay network structures. MMT structures can play a compatibilization role by making a bridge between two immiscible polymers or suppress the coalescence of droplets, which is consistent with the reduction in the droplet size of the dispersed phase as a function of MMT content (Fig. 4). Moreover, interactions between clays and PLA/PCL blends immobilize the polymer chains and increase toughness. Therefore, solid-like behavior develops up to a certain strain amplitude (crossover strain amplitude γ_{0c}).

Lissajous curves (normalized stress vs. normalized strain) were obtained as a function of strain amplitudes at various MMT concentrations (1, 2, and 4 phr) in Fig. 7. Based on the Lissajous plot's concept, a pure elastic material shows a straight line, while a perfect viscous material exhibits a circular shape; therefore, a viscoelastic material response is somewhat between a straight line and a circle [32]. The Lissajous loops showed an ellipsoidal shape and were

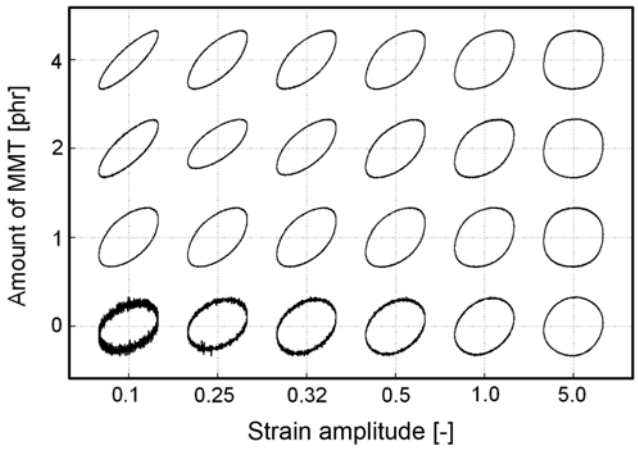

Fig. 7. Lissajous plots of PLA/PCL/MMT blends at different strain amplitudes and the amount of MMT at a fixed frequency, ω=1 rad/s at 190 °C.

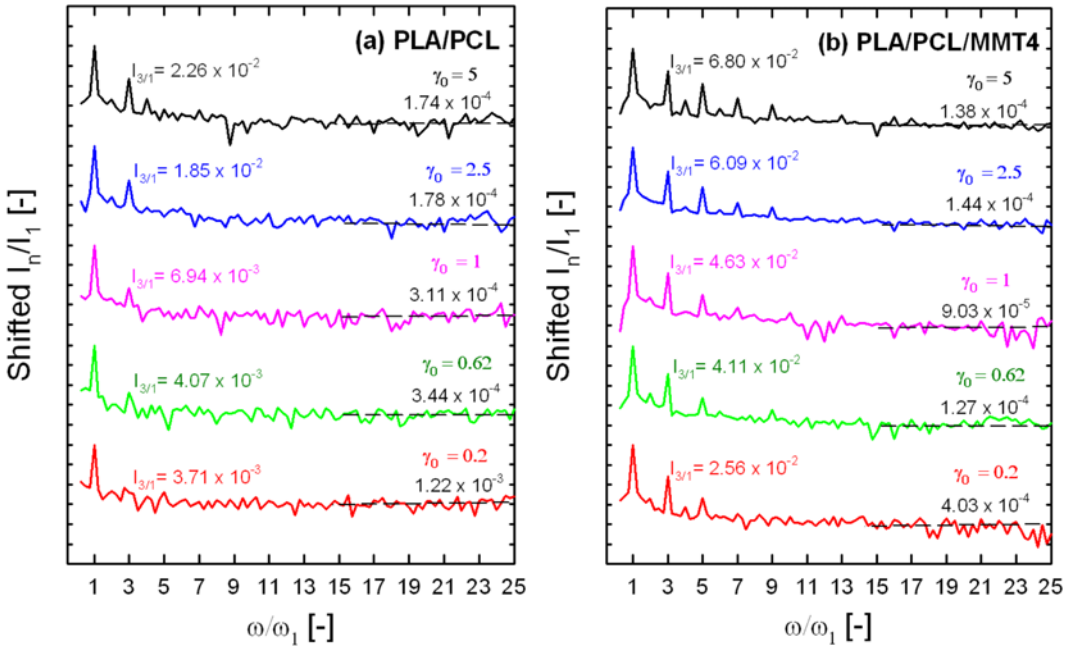

Fig. 8. The Fourier spectra at various strain amplitudes (γ_0=0.2, 0.62, 1.0, 2.5, and 5.0) as a function of normalized frequency by mechanical excitation frequency ($\equiv\omega/\omega_1$) for (a) PLA/PCL and (b) PLA/PCL/MMT4 blend. The odd higher harmonics increased with increasing strain amplitude. The noise level was obtained by averaging the normalized intensity from ω/ω_1=15 to 25 (medium-dash line). The $I_{3/1}$ value was distinct when compared with noise level, especially PLA/PCL/MMT4 blend. In case of PLA/PCL blend, the $I_{3/1}$ value is very similar like noise level at low strain amplitude.

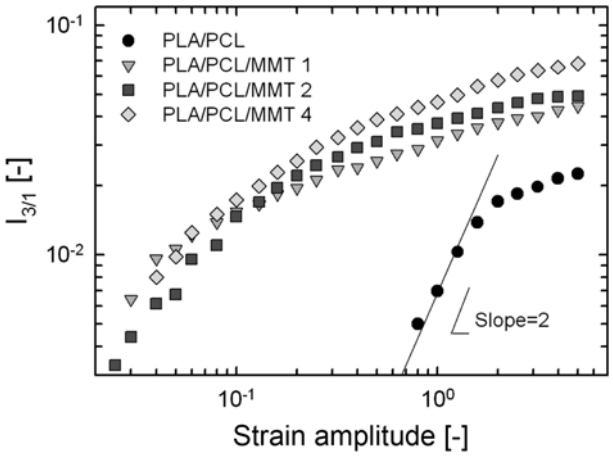

Fig. 9. The normalized 3rd harmonics ($I_{3/1}$) of PLA/PCL, PLA/PCL/MMT1, PLA/PCL/MMT2, PLA/PCL/MMT4 blends as a function of strain amplitude at a fixed frequency of 1 rad/s and 190 °C.

closer to a straight line at small strain amplitudes, signifying the elastic contribution. These ellipsoidal loops become more circular with increasing strain amplitude as a consequence of viscous-like-behavior at large strain amplitudes. Conversely, the Lissajous loops became more distorted when the MMT concentration increased. These distorted shapes came from introduction of a new phase (clay) to the polymeric matrix.

2. FT-rheology

The Lissajous pattern is useful for understanding the nonlinear response of a complex fluid, but its usefulness is limited because it provides the information in terms of shape but not numbers. For better quantification of non-linear viscoelastic behavior, the relative intensity of third harmonics [$I_{3/1} \equiv I(3\omega)/I(\omega)$, where ω is the excitation frequency] of blend systems was investigated through FT-Rheology. The relative third higher harmonics ($I_{3/1}$) are the most representative and significant among the odd higher harmonics [27,33]. Fig. 8 illustrates how stress curves as a function of time are converted to the intensity curve as a function of frequency by using the Fourier transform (FT). The relative intensity of third harmonics ($I_{3/1}$) at all strain amplitudes was acquired and then depicted as a function of strain amplitude to quantify the nonlinear viscoelasticity of PLA/PCL blends. Fig. 9 illustrates the ($I_{3/1}$) of blends as a function of strain amplitude. MMT concentration dependency of nonlinearity was quite remarkable, suggesting that FT-rheology measurements are more sensitive to internal changes in the polymer blends. These results are consistent with those of Lim et al. [34] who found that the $I_{3/1}$ of PCL nanocomposites increased when multiwall nanocarbon tube (MWNT) and clay (organomodified MMT) weight percent increased. This enhancement in nonlinearity could be due to exfoliation structures and clay alignments with normal direction of shear flow [35].

3. LAOS Tests of PLA/PCL/mLLDPE/MMT Blends

Rheological enhancement upon MMT loading was also repeated when mLLDPE was added to the blend systems as an impact modi-

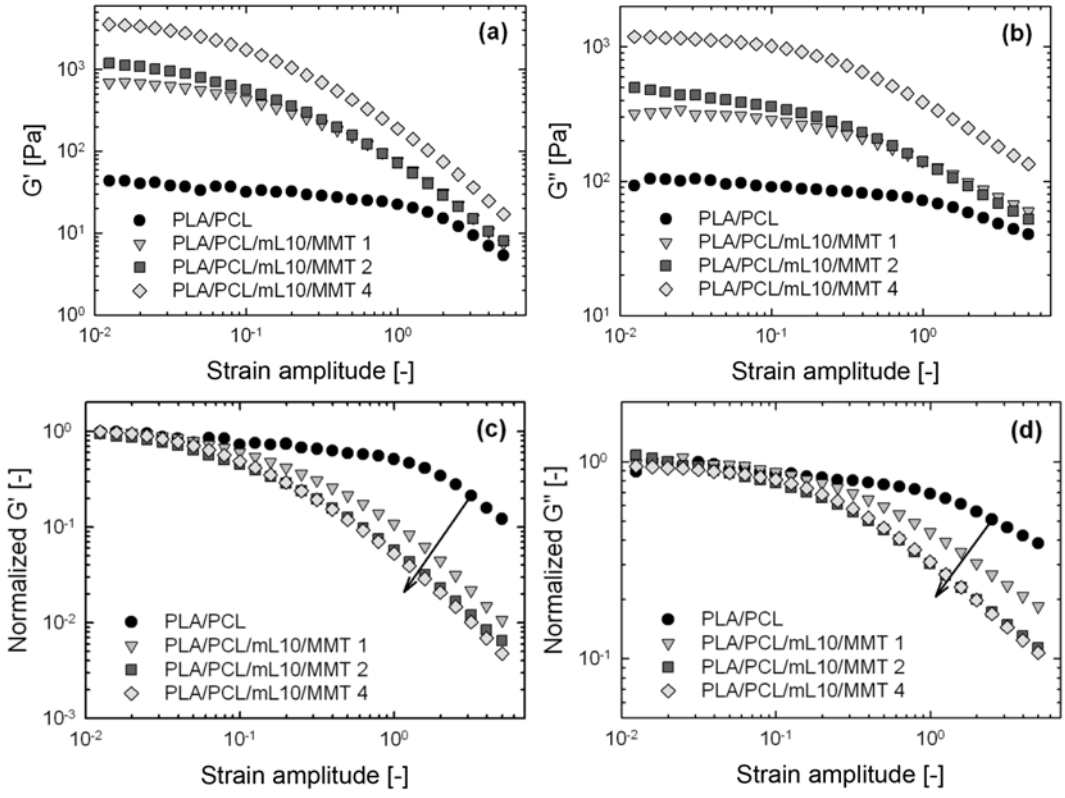

Fig. 10. Effect of MMT concentrations on dynamic (a) storage modulus $G'(\gamma_0)$, (b) loss modulus $G''(\gamma_0)$, (c) normalized storage modulus [$\equiv G'(\gamma_0)/G'$ (linear regime)], and (d) normalized loss modulus [$\equiv G''(\gamma_0)/G''$ (linear regime)] of PLA/PCL/mLLDPE blends at a fixed frequency, ω=1 rad/s and 190 °C.

fier. As shown in Fig. 10(a) and 10(b), both G′ and G″ increased with increasing MMT. Fig. 10(c) and 10(d) show the normalized storage and loss modulus of the PLA/PCL/mLLDPE blends as the MMT content increases. These values differed from those obtained using the PLA/PCL/MMT blends (see Fig. 5(c) and 5(d)). As MMT concentration increased in the PLA/PCL/mLLDPE blends, both normalized G′ and G″ showed stronger strain thinning behavior (see Fig. 10(c) and 10(d)). As shown in Fig. 11, the crossover strain amplitude (γ_{0c}) occurred at the same strain amplitude of 0.32 for all MMT content (see arrow in Fig. 11). These results were quite different from those obtained for the PLA/PCL/MMT blends (see Fig. 6). Overall, these findings indicate that mLLDPE is the governing factor controlling the viscoelasticity of PLA/PCL/MMT blends, since the crossover point remains unchanged when the MMT concentration increases at fixed mLLDPE contents. As discussed in the previous section, the elastic-viscous transition is governed by amount of MMT in PLA/PCL/MMT blends. In PLA/PCL/mLLDPE blends, polymer systems appeared to be filled well-enough by mLLDPE (10 phr). Therefore, incorporation of MMT exhibited no contribution to the control of the elastic-viscous behavior, but did influence the magnitude of enhancements. In other words, mLLDPE is the dominant phase leading to formation of solid-like structures; therefore, MMT loadings do not affect the solid-like structure of the blends.

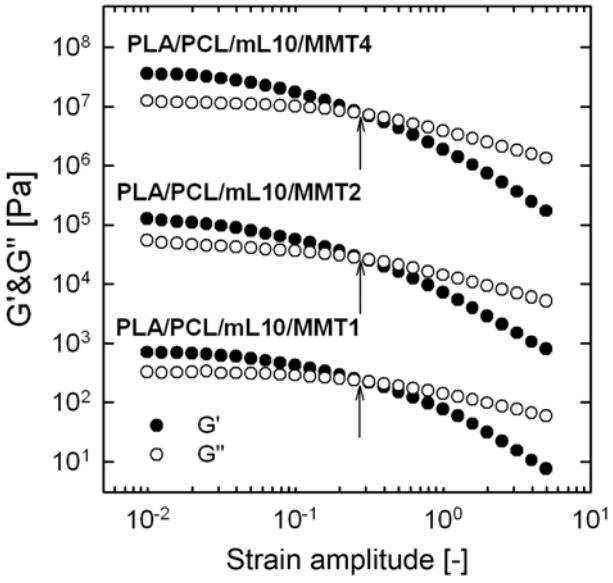

Fig. 11. Observation of crossover points in PLA/PCL/MMT/mLLDPE blends at frequency 1 rad/s and 190 °C. The moduli data have been multiplied by 10^0 for PLA/PCL/mL10/MMT1, 10^2 for PLA/PCL/mL10/MMT2, and 10^4 for PLA/PCL//mL10/MMT4, respectively, for clarity of presentation.

For further investigation, the effects of addition of mLLDPE to the blends on nonlinear rheological properties were evaluated through comparison of the $I_{3/1}$ of PLA/PCL/MMT with and without mLLDPE (Fig. 12(a), 12(b), and 12(c)). The nonlinearity of PLA/PCL/MMT/mLLDPE was found to be larger than that of PLA/PCL/MMT due to the solid-like behavior of mLLDPE (higher viscosity than

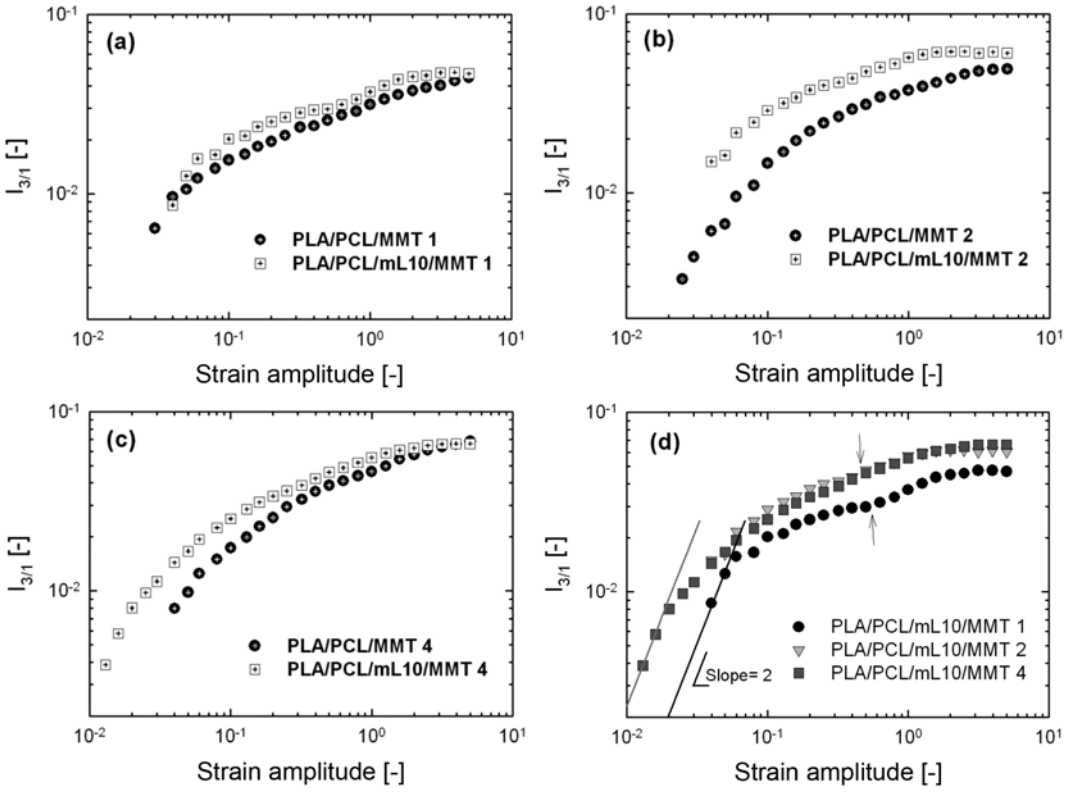

Fig. 12. Comparison of normalized 3rd harmonics of PLA/PCL/MMT with mLLDPE added counterparts at a fixed frequency of 1 rad/s and 190 °C. (a) PLA/PCL/mL10/MMT1, (b) PLA/PCL/mL10/MMT2, (c) PLA/PCL/mL10/MMT4 (d) The normalized 3rd harmonics ($I_{3/1}$) of PLA/PCL/mL10 blends with various MMT concentrations, 1, 2, and 4 phr (PLA/PCL/mL10/MMT1, PLA/PCL/mL10/MMT2, and PLA/PCL/mL10/MMT4).

PLA and PCL). Fig. 12(d) shows the effects of MMT on PLA/PCL/mLLDPE. The magnitude of the $I_{3/1}$ curves did not significantly change as the MMT content changed from 2 to 4 phr. When mLLDPE was added to PLA/PCL, the magnitude of nonlinearity increased when compared with those of counterpart blend systems without mLLDPE. Interestingly, the nonlinearity curve showed a double-arc-shaped behavior, with the local minimum point occurring when there was a low MMT content. This may have been a result of the addition of another immiscible phase (mLLDPE) to the PLA/PCL/MMT blends. This behavior gradually disappeared when MMT content increased up to 4 phr, producing a curve without local minimum. Previous study by Balakrishnan et al. [36] showed MMT layers intercalated in PLA matrix in case of PLA/LLDPE/MMT blends. Therefore, it can be referred that MMT layers intercalated or exfoliated in either phases of PLA or PCL in the current system as well. These phenomena explain why the $I_{3/1}$ curves of the PLA/PCL/mL/MMT blends show a double-phase-like shape (see Fig. 12(a) and (b)). Possible migration of MMT layers toward mLLDPE phase at higher concentrations could be the reason for the perfect shape of $I_{3/1}$ curve of PLA/PCL/mL/MMT at 4 phr. Namely, extra MMT play role in compatibilizing the PLA/PCL and mLLDPE phase. Therefore, the $I_{3/1}$ curve of PLA/PCL/mL/MMT at 4 phr shows an almost single-phase shape (see Fig. 12(c)) concurrent with the results of PLA/PCL/MMT blends. However, the amount of MMT in intermediate phases is not sufficient to participate in solid-like structure formation. As a result, the elastic-viscous transition point remains unchanged at all MMT concentrations. This phase separation can be seen in heterogeneous SEM images of blends containing mLLDPE. The formation of voids when there is low MMT content indicates incompatibility of mLLDPE with the PLA/PCL blend (see Fig. 13(d), 13(e), and 13(f)). Furthermore, it has been reported that heterogeneous morphology can lead to the formation of fibrils or elongated structures [37]. These elongated structures have also been observed in PLA/PCL/MMT/mLLDPE blends at low MMT concentrations as shown in Fig. 13(a), 13(b), and 13(c). Interestingly, when the MMT content increased, less void space formation was observed in a relatively small area and no elongated structures were observed in a relatively large area (see Fig. 13(c) and 13(f), MMT 4 phr), suggesting that MMT has a compatibilizing effect on PLA/PCL/mLLDPE ternary blends. It is known that organomodified MMT can be used to increase the affinity of immiscible PLA/PCL blends through linkage of its hydrophilic tail to PLA and its hydrophobic tail to PCL. At low MMT concentrations, the surface areas of MMTs are not large enough to react with both the PLA/PCL blend and mLLDPE. Thus, $I_{3/1}$ curves showed two-phase-like behavior in cases in which mLLDPE contained low levels of MMT (MMT 1 and 2 phr). On the contrary, at higher MMT concentrations (4 phr) the MMT surface area was sufficient to react with both PLA/PCL and mLLDPE, which led to $I_{3/1}$ curves without a local minimum point (see Fig. 12).

CONCLUSION

SAOS (large amplitude oscillatory shear) and LAOS (large amplitude oscillatory shear) tests were conducted to evaluate the nonlinear rheological properties of PLA/PCL blends with and without MMT. The results showed that OMMT (clay) loading enhanced elastic-like-behavior at low frequency in the SAOS test, while it enhanced strong strain thinning behavior and increased nonlinearity in the LAOS test. FT-Rheology measurements were used to quantify the nonlinear viscoelastic properties of the blends. Rheological enhancements of blends were consistent with SEM images of blends, which showed a decrease in droplet size of the PCL dispersed phase. Three possible mechanisms were offered for decrease in droplet sizes: (1) coalescence of droplets suppressed whereas clays acted as barrier, (2) interfacial adhesions enhanced by decreasing interfacial tensions, and (3) preferential distribution of clays in one of the phases and changing the viscosity ratio of the blends. Furthermore, the relative

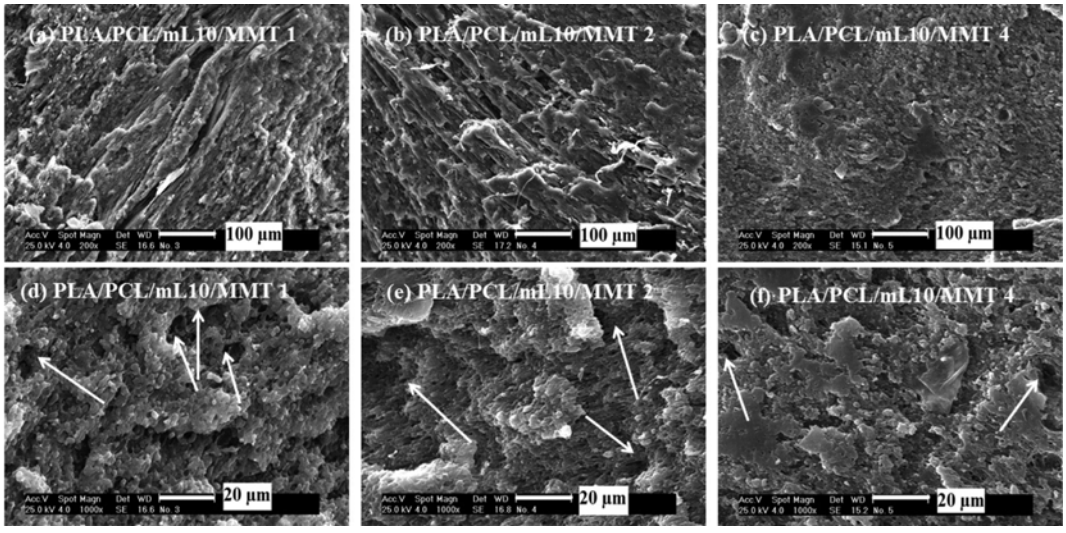

Fig. 13. SEM images of (a) PLA/PCL/mL10/MMT1, (b) PLA/PCL/mL10/MMT2 and (c) PLA/PCL/mL10/MMT4 blends with relatively large area (scaling bar is 100 μm) and SEM images of (d) PLA/PCL/mL10/MMT1, (e) PLA/PCL/mL10/MMT2 and (f) PLA/PCL/mL10/MMT4 blends with relatively small area (scaling bar is 20 μm). SEM images (a)-(c) are 5 times larger than SEM images (d)-(f). Fibrillar structure can be seen in (a) and (b). In (d)-(f), voids spaces are pointed out by arrows in small scale SEM images.

intensity of the 3rd harmonics ($I_{3/1}$) of PLA/PCL/MMT blends with and without mLLDPE was also compared. This comparison revealed that a two-phase-shaped curve with a local minimum was produced in cases in which mLLDPE was contained at low level of MMT and was improved to a perfect-shaped curve when the MMT content was 4 phr. These findings indicate that OMMT acted as a compatibilizer between mLLDPE and the PLA/PCL blend. Overall, the results of this study indicated that LAOS tests could be useful tools to investigate the morphology of polymer blends systems as well as the SAOS test; however, further investigations of the LAOS test of polymer blends systems are necessary.

ACKNOWLEDGEMENTS

This work was supported by a 2-Year Research Grant of Pusan National University.

REFERENCES

1. S. S. Ray and M. Bousmina, *Prog. Mater. Sci*., **50**, 962 (2005).
2. S. S. Ray and M. Okamoto, *Prog. Polym., Sci*., **28**, 1539 (2003).
3. S. Jacobsen, P. Degee, H. G. Fritz, P. Dubois and R. Jerome, *Polym. Eng. Sci.*, **39**(7), 1311 (1999).
4. J. S. Jung, X. Liu and H. S. Choi, *Korean Chem. Eng. Res.*, **47**(1), 59 (2009).
5. R. M. Rasal and D. E. Hirt, *J. Biomed. Mater. Res. Part A*., **88A**, 1079 (2008).
6. C. C. Chen, J. Y. Chueh, H. Tseng, H. M. Huang and S. Y. Lee, *Biomaterials*., **24**, 1167 (2003).
7. Y. Di, S. Iannace, E. Di Maio and L. Nicolais, *J. Polym. Sci. Polym. Phys.*, **41**, 670 (2003).
8. H. Liu, C. Han and L. Dong, *J. Appl. Polym. Sci*., **115**, 3120 (2010).
9. M. Tortora, V. Vittoria, G. Galli, S. Ritrovati and E. Chiellini, *Macromol. Mater. Eng*., **287**, 243 (2002).
10. J. D. Ferry, *Viscoelastic properties of polymers*, Wiley, New York (1980).
11. R. B. Bird, R. C. Armstrong and O. Hassager, *Dynamics of polymeric liquids*, Wiley, New York (1987).
12. D. Wu, Y. Zhang, M. Zhang and W. Zhou, *Eur. Polym. J.*, **44**, 2171 (2008).
13. D. Wu, Y. Zhang, L. Yuan, M. Zhang and W. Zhou, *J. Polym. Sci.: Part B: Polym. Phys.*, **48**, 756 (2010).
14. S. S. Sabet and A. A. Katbab, *J. Appl. Polym. Sci.*, **111**, 1954 (2009).
15. J. Ahmed, S. K. Varshney and R. Auras, *J. Food Sci.*, **75**, 17 (2010).
16. K. Li, J. Peng, L. S. Turng and H. X. Huang, *Adv. Polym. Technol*., **30**, 150 (2011).
17. R. Krishnamoorti and E. P. Giannelis, *Macromolecules*., **30**, 4097 (1997).
18. S. G. Hatzikiriakos, *Polym. Eng. Sci.*, **40**, 2279 (2000).
19. C. Gabriel, E. Kokko, B. Lofgren, J. Seppala and H. Munstedt, *Polymer.*, **43**, 6383 (2002).
20. T. Neidhofer, S. Sioula, N. Hadjichristidis and M. Wilhelm, *Macromol. Rapid. Commun.*, **25**, 1921 (2004).
21. K. Hyun, S. H. Kim, K. H. Ahn and S. J. Lee, *J. Non-Newt. Fluid Mech.*, **107**, 51 (2002).
22. K. Hyun, J. G. Nam, M. Wilhelm, K. H. Ahn and S. J. Lee, *Korea-Aust. Rheol. J.*, **15**, 97 (2003).
23. S. H. Kim, K. Hyun, T. S. Moon, T. Mitsumata, J. S. Hong, K. H. Ahn and S. J. Lee, *Polymer.*, **46**, 7156 (2005).
24. M. Sugimoto, T. Koizumi, T. Taniguchi, K. Koyama, K. Saito, D. Nonokawa and T. Morita, *J. Polym. Sci.: Part B: Polym. Phys.*, **47**, 2226 (2009).
25. I. Vittorias, M. Parkinson, K. Klimke, B. Debbaut and M. Wilhelm, *Rheol. Acta*, **46**, 321 (2007).
26. I. Vittorias, D. Lilge, V. Baroso and M. Wilhelm, *Rheol. Acta*, **50**, 691 (2011).
27. K. Hyun, M. Wilhelm, C. Klein, K. S. Cho, J. G. Nam, K. H. Ahn, S. J. Lee, R. Ewoldt and G. H. McKinley, *Prog. Polym. Sci*., **36**, 1697 (2011).
28. M. Wilhelm, D. Maring and H. Wolfgang Spiess, *Rheol. Acta*, **37**, 399 (1998).
29. S. Filipe, M. T. Cidade, M. Wilhelm and J. M. Maia, *J. Appl. Polym. Sci.*, **99**, 347 (2004).
30. C. Carotenuto, M. Gross and P. L. Maffetone, *Macromolecules.*, **41**, 4492 (2008).
31. D. Wu, L. Wu, L. Wu and M. Zhang, *Polym. Degrad. Stabil.*, **91**, 3149 (2006).
32. R. H. Ewoldt, A. E. Hosoi and G. H. McKinley, *J. Rheol*., **52**, 1427 (2008).
33. M. Wilhelm, P. Reinheimer and M. Ortseifer, *Rheol. Acta*, **38**, 349 (1999).
34. H. T. Lim, K. H. Ahn, S. J. Lee, J. S. Hong and K. Hyun, Submitted *J. Rheol.* (2012).
35. K. Hyun, H. T. Lim and K. H. Ahn, *Korea-Aust. Rheol. J.*, **24**, 113 (2012).
36. H. Balakrishnan, A. Hassan, M. U. Wahit, A. A. Yussuf and S. B. K. Razak, *Mater. Des*., **31**, 3289 (2010).
37. M. D. Cardenas, R. Perera, N. Villarreal, C. Rosales and J. M. Pastor, *J. Appl. Polym. Sci.*, **106**, 2298 (2007).